Title	POSITIVE PION PRODUCTION BY 185 MEV PROTONS
Author(s)	Kume, Kenji
Citation	大阪大学, 1976, 博士論文
Version Type	VoR
URL	https://hdl.handle.net/11094/1448
rights	
Note	

POSITIVE PION PRODUCTION BY 185 MEV PROTONS

KENJI KUME

(DOCTOR THESIS)

DEPARTMENT OF PHYSICS, OSAKA UNIVERSITY

Contents

Abstract

Positive pion production by 185 MeV protons on ^{12}C is studied theoretically. We perform the phenomenological analysis of the experimental data with the distorted wave approximation. It is shown that the final state interaction, especially, the off-shell behavior of the pion-nucleus optical potential is essential to understand this particular process. In the previous calculations of ^{12}C(p, π^+)^{13}C reaction cross section, the theoretical values are an order of magnitude larger than the experimental data or more, when the Kisslinger-type pion-nucleus optical potential is employed. It is shown that this difficulty is due to the wrong off-shell behavior of the Kisslinger-potential. We adopt here a Gaussian-type cut-off function for reducing the off-shell contribution of the p-wave pion-nucleus interaction in the Kisslinger-model. As a result, the pion elastic scattering and the ^{12}C(p, π^+)^{13}C reaction cross section can be consistently explained.

1. Introduction

Pion induced nuclear reactions have extensively investigated in the low as well as the intermediate energies (pion kinetic energy $T_\pi \lesssim 300$ MeV) to determine the interaction of pion with nuclei and to clarify the nuclear structure with this interaction[1-6]. These reactions involve the pion capture, phenomena concerning the pionic atom, elastic, inelastic and charge exchange reactions of pions by complex nuclei,etc. In these pion induced reactions, the excitation of various modes of the nucleon or the nuclear motion is possible.

Apart from the study of the nuclear structure, the investigation of the pion-nucleus interaction itself is interesting. There is a strong resonance in the pion-nucleon P_{33} channel with the mass $m_\Delta = 1236$ MeV, and the s and p-wave scatterings are dominant in the low energy. Because of these, the pion-nucleon interaction is quite different from the nucleon-nucleon interaction, and these properties are revealed in pion-nucleus interaction. One of the main problems in the low-energy pion-nucleus physics is the determination of the pion-nucleus optical potential.

In 1955, Kisslinger[7] has proposed a pion-nucleus optical potential which takes into account the s and p-wave character of the low-energy pion-nucleon scattering. This semi-phenomenological potential has succeeded to explain the low and intermediate-energy pion-nucleus elastic scattering in various nuclei.

Recently, however, the following difficulty arises in the theoretical analysis of the pion production reaction by 185 MeV protons on nuclei.

$$p + (A, Z) \longrightarrow (A+1, Z) + \pi^+$$
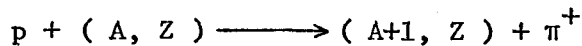
Rost and Kunz[8], and Keating and Wills[9] have calculated the cross

section of this (p, π^+) reaction on ^{12}C in the distorted wave

approximation, and have shown that the theoretical values are

an order of magnitude larger or more, compared with the experimental data

[10-12]. They have used the phenomenological optical potential for

the proton and the Kisslinger-type potential for the pion.

The parameters of these potentials are chosen so as to fit to the

respective elastic scatterings. The calculated cross sections are

shown to be strongly dependent upon the choice of the pion optical

potential. Several modifications of the Kisslinger-potential are

tried, but the pion elastic scattering and the $^{12}C(p, \pi^+)^{13}C$ reaction

cross section can not be explained consistently. Keating and Wills[9]

have concluded that the cause of the trouble would consist either

in the pion optical potential or in the distorted wave approximation

itself. For these difficulties, Miller[13] have reexamined the parameter

search for the Kisslinger-potential to fit the elastic scattering

and the (p, π^+) reaction cross section. He obtained the potential-

parameters which can fit to both of these experimental data. But his

parameters are quite different from the theoretical value which is

given by the pion-nucleon phase shifts in the multiple scattering

theory. It is hard, therefore, to accept these parameters. Recently,

Miller and Phatak[14] have calculated the $^{12}C(p, \pi^+)^{13}C$ reaction cross

section by the separable potential proposed by Landau et al.[15,16]. The

results are in a good agreement with the experimental data of the elastic

scattering and the (p, π^+) reaction, but the parameters adopted for

the nuclear form factor are too large. Because of these difficulties,

there arises a doubt that the original parametrization of the Kisslinger-potential might be wrong.

The purpose of the present thesis is to investigate the above mentioned theoretical difficulties in understanding the (p, π^+) reaction cross section. The trouble comes from the particular nature of the (p, π^+) reaction. In (p, π^+) reaction, the momentum of the incident proton is about $p \cong 560$ MeV/c in the CM system of the proton and the target nucleus, while for the pion $k \cong 100$ MeV/c. If we assume the proton and the pion to be the free particles, the momentum of the transferred neutron amounts to 460 MeV/c, which is far above the nuclear Fermi momentum. Since such a high-momentum component is very small in the nucleus, the cross section for this process is expected to be small. However, the proton and the pion are not free but interact with nucleus. They are described by the distorted waves and have various momentum components. The low-momentum neutrons can be transferred to the nucleus if the highly off-shell pion is emitted at the pion-nucleon vertex. Therefore, the cross section of this (p, π^+) reaction is expected to be strongly dependent upon the momentum distribution of the pion distorted wave. Thus the (p, π^+) reaction cross section is sensitive to the off-shell behavior of the pion-nucleus optical potential. In contrast with this, the elastic scattering is almost determined by the on-shell part of the pion potential. Then it is probable that the failure of the Kisslinger-potential in the calculation of the (p, π^+) reaction is due to the wrong off-shell behavior of this potential.

In this thesis we give the general formula for the (p, π^+) reaction cross section by expanding the transition matrix elements into multipole

series. In order to modify the off-shell behavior of the Kisslinger-type pion potential, we must deal with the non-local potential. Therefore we have obtained the pion wave function in the momentum space by directly solving the integral equations. The effects of the nuclear recoil, which are neglected in the previous calculations, are taken into account by changing the pion momentum effectively.

We will show that the off-shell extrapolation of the p-wave pion-nucleon interaction in the Kisslinger-potential is wrong. Introducing the phenomenological cut-off function, we have improved the off-shell behavior of the Kisslinger-potential. This cut-off procedure scarcely affects the cross section of pion elastic scattering, but appreciably reduces the absolute value of the (p, π^+) reaction cross sections. Thus we can explain the pion elastic scattering and the $^{12}C(p, \pi^+)^{13}C$ reaction cross section consistently.

In section 2, we describe the mechanism of the (p, π^+) reaction qualitatively, in order to clarify the problem involved. In section 3, the formulas for the differential cross section of the (p, π^+) reaction are given, and the recoil correction in the nuclear matrix element is also studied. In section 4, we describe the proton and the pion optical potentials adopted in our calculations and propose a modification of the off-shell extrapolation in the Kisslinger-potential. The results of the numerical calculations are given and are discussed in section 6. In section 7, we summarize the results obtained in our analysis. We adopt the natural units $\hbar = c = 1$ in this thesis throughout.

2. Plane wave approximation

In this section we describe the (p, π^+)reaction in the plane wave approximation and give the qualitative arguments which are helpful to clarify the problem involved. The interaction Hamiltonian of the pion-nucleon interaction is assumed to be the pseudo-vector coupling and it is given by in non-relativistic limit as[17]

$$H_I = -\sqrt{4\pi}\,\frac{f}{\mu}\int \psi_N^\dagger(r)\,(\sigma\nabla_\pi)(\tau\,\phi(r))\,\psi_N(r)\,dr \qquad (2.1)$$

where $\phi(r)$ and $\psi_N(r)$ are the pion and the nucleon field operators, respectively. The f is the pion-nucleon coupling constant ($f^2 = 0.083$) and μ the pion mass. The spin and the isospin operators of the nucleon are denoted as σ and τ, respectively. The gradient operator ∇_π operates only on the pion coordinate. The (p, π^+) reaction cross section is then given by

$$d\sigma = 2\pi\,\frac{1}{j_{flux}}\sum_f \overline{\sum_i}\,\delta(E_i + E_p - E_f - E_\pi)|\langle f|H_I|i\rangle|^2 \qquad (2.2)$$

where j_{flux} is the flux of the incident proton, $|i\rangle$ the initial state with proton and the target nucleus, and $|f\rangle$ the final state with the emitted pion and the residual nucleus. The total energies of the pion and the proton are denoted by E_π and E_p, and E_i and E_f are the same for the target and the residual nucleus. In eq. (2.2), the square of the transition matrix is averaged over the initial state and summed over the final state. We assume that the pion and the proton are described by the plane wave. In the case of the spin-zero target nucleus, the differential cross section for (p, π^+) reaction is

given by,

$$\left(\frac{d\sigma}{d\Omega}\right)_{pw} = 2 \left(\frac{f}{\mu}\right)^2 \frac{E_p}{p} k^3 (2I+1) |F(q)|^2 \qquad (2.3)$$

$$F(q) = \int_0^\infty j_\ell(qr) R_B(r) r^2 dr \qquad (2.4)$$

$$q = |k - p| \quad .$$

Here, the target nucleus is assumed to be the closed shell, and the residual nucleus consists of the closed core plus one neutron state with orbital and total angular momenta ℓ and I, respectively. Its radial wave function is denoted as $R_B(r)$. The $j_\ell(qr)$ is the spherical Bessel function. The p and k are the momenta of the incident proton and the emitted pion, respectively. The cross section is then directly proportional to the Fourier-transform of the bound-neutron wave function. In the (p, π^+) reaction, the momentum q of the transferred neutron is especially large. Even when the pion is emitted in the forward direction, q is about 460 MeV. The calculated cross section of the $^{12}C(p, \pi^+)^{13}C$ (ground state) is shown in Fig. 1 with the experimental values by Dahlgren et al.[10]). The result in the plane wave approximation is smaller than the experimental data by an order of magnitude. This is due to the fact that the high-momentum component of a nuclear single particle state is very small.

The importance of the initial or the final state interactions in the (p, π^+) reaction can be seen as follows. The nuclear form factor F(q) in eq. (2.4) is replaced by

$$F(|p - k|) \longrightarrow \int \phi_\pi^{*k}(k') \phi_p^{*P}(p') F(|p' - k'|) dk' dp' \qquad (2.5)$$

in the distorted wave approximation. Here, $\phi_\pi^{k}(k')$ and $\phi_p^{P}(p')$ are the

distorted waves of the pion and the proton in the momentum space,

respectively. The nuclear form factor $F(|k' - p'|)$ has the peak where

the momentum transfer $|k' - p'| \lesssim 250\text{MeV}$. Therefore the behavior of

the pion and the proton wave functions in this domain mainly determines

the above integral. In other words, the high-momentum components in

the respective wave functions are important. As will be shown in

section 6, the effects of the pion distorted wave, especially, the

high-momentum component, are essential in understanding the (p, π^+)

reaction cross section, and these are closely related to the off-shell

behavior of the pion-nulceus optical potential. In momentum space,

the Klein-Gordon equation in the potential $\langle k'|V_\pi(E_\pi)|k''\rangle$ is given by

$$(k'^2 - k^2)\phi_\pi^{k}(k') = -2 E_\pi \int \langle k'|V_\pi(E_\pi)|k''\rangle \phi_\pi^{k}(k'') dk'' \qquad (2.6)$$

In the Born approximation, the off-shell component $|k| \neq |k'|$ of the

pion wave function is proportional to

$$\phi_\pi^{k}(k') \propto \frac{\langle k'|V_\pi(E_\pi)|k\rangle}{k'^2 - k^2} \qquad (2.7)$$

Thus the cross section of the (p, π^+) reaction is expected to be

sensitive to the off-shell behavior of the pion-nucleus optical

potential.

3. Formulation for the (p, π^+) reaction cross section

In this section, we formulate the (p, π^+) reaction cross section for the numerical calculations including the nuclear recoil effects.

3.A. Kinematics

First of all, we describe the kinematics of the reaction, as follows. We denote the four momenta of the incident proton, emitted pion, target and the residual nucleus as P_p, P_π, P_T and P_R, respectively. The Lorentz-invariant variable s, which represents the square of the total energy in the CM system of the proton and the target nucleus, is defined by

$$s = (P_p + P_T)^2$$
$$= (P_\pi + P_R)^2 .$$

(3.1)

In the laboratory system, s is given by

$$s = (M_N + m_p)^2 + 2 M_N T_p ,$$

(3.2)

where m_p and M_N are the masses of the proton and the target nucleus, respectively, and T_p the proton kinetic energy in the laboratory system. The momenta of the incident proton p and the emitted pion k in the proton or the pion-nucleus CM system are given by

$$|p| = \left[\frac{1}{s} \left(\frac{s + m_p^2 - M_N^2}{2} \right)^2 - m_p^2 \right]^{1/2} ,$$

(3.3)

$$|k| = \left[\frac{1}{s} \left(\frac{s + \mu^2 - M_N^{*2}}{2} \right)^2 - \mu^2 \right]^{1/2} ,$$

(3.4)

where μ is the pion mass and M_N^* the mass of the residual nucleus. In the reaction $^{12}C(p, \pi^+)^{13}C$ (ground state), the numerical values are

$$P = 561.9 \; MeV$$
$$k = 101.7 \; MeV \; . \tag{3.5}$$

3.B. Cross section for the (p, π^+) reaction

In this subsection we derive a formula for the differential cross section of the (p, π^+) reaction. We expand the initial and the final state by the eigenstates of the total angular momentum. As was given in section 2, the interaction Hamiltonian of the pion and the nucleon is

$$H_I = -\sqrt{4\pi} \frac{f}{\mu} \int \psi_N^\dagger(r) (\sigma \nabla_\pi)(\tau \phi(r)) \psi_N(r) \, dr . \tag{3.6}$$

It is necessary to evaluate the following transition matrix element.

$$\langle f | H_I | i \rangle = \langle k; I I_z(-) | H_I | p\sigma; I_0 I_{0z} (+) \rangle \tag{3.7}$$

Here, the initial state vector $| p\sigma; I_0 I_{0z} (+) \rangle$ with the outgoing-wave boundary condition is represented by the proton momentum p, spin projection σ, the spin I_0 and its projection I_{0z} of the target nucleus. If it is necessary the same symbol I_0 represents the whole set of the quantum numbers characterizing the target nucleus. Similarly the final state vector $| k; I I_z(-) \rangle$ with the incoming-wave boundary condition is specified by the pion momentum k and the residual nuclear state with spin I and its projection I_z. These state vectors are normalized as follows:

$$\langle \mathbb{P}\sigma;\, I_0 I_{0z}\,(+)|\mathbb{P}'\sigma';\, I_0' I_{0z}'\,(+)\rangle = \delta(\mathbb{P}-\mathbb{P}')\,\delta_{\sigma\sigma'}\,\delta_{I_0 I_0'}\,\delta_{I_{0z} I_{0z}'} \,, \qquad (3.8)$$

$$\langle \mathbb{K};\, I\, I_z\,(-)|\mathbb{K}';\, I'\, I_z'\,(-)\rangle = \delta(\mathbb{K}-\mathbb{K}')\,\delta_{II'}\,\delta_{I_z I_z'} \,. \qquad (3.9)$$

They are expanded in terms of the eigenstates of the parity and the total angular momentum,

$$|\mathbb{P}\sigma;\, I_0 I_{0z}\,(+)\rangle = \sum_{\ell_p m_p} i^{-\ell_p}\, Y_{\ell_p m_p}^{*}(\hat{\mathbb{P}}) \sum_{\substack{j_p, m_j \\ J,M}} (\ell_p\, \tfrac{1}{2}\, m_p\, \sigma|j_p\, m_j)$$

$$\times (j_p\, I_0\, m_j\, I_{0z}|J M)\, |J M,\, c\,(+)\rangle \,, \qquad (3.10)$$

$$|\mathbb{K};\, I\, I_z\,(-)\rangle = \sum_{\substack{\ell_\pi, m_\pi \\ J',M'}} i^{\ell_\pi}\, Y_{\ell_\pi m_\pi}^{*}(\hat{\mathbb{K}})\, (\ell_\pi\, I\, m_\pi\, I_z|J'M')$$

$$\times |J'M';\, \ell_\pi\, I\,(-)\rangle \,. \qquad (3.11)$$

Here, ℓ_p and j_p are the orbital and the total angular momenta of the proton, respectively, and $Y_{\ell_p m_p}$ is the spherical harmomic. The state vector with spin J and its projection M is denoted as $|JM,\ c(+)\rangle$, and the c represents the channel index,

$$c = \{\ell_p,\, j_p,\, I_0\} \,, \qquad (3.12)$$

which specifies the incident channel. In eq. (3.11), ℓ_π is the orbital angular momentum of the emitted pion and $|J'M';\ \ell_\pi\, I(-)\rangle$ is the eigenstate of the total angular momentum J' and its projection M'. The channel index (ℓ_π, I) represents the exit channels. Substituting eqs. (3.10) and (3.11) into the transition matrix element

(3.7), we have

$$\langle K; I\, I_z\, (-) \,|\, H_I \,|\, \mathcal{P}\sigma; I_0\, I_{0z}(+)\rangle$$

$$= \sum_{\substack{\ell_p,\, j_p,\, \ell_\pi,\, J \\ m_\pi,\, m_p,\, m_j,\, M}} i^{\ell_p - \ell_\pi} (\ell_p\, \pm\, m_p\, \sigma \,|\, j_p\, m_j)(j_p\, I_0\, m_j;\, I_{0z}\,|\, JM)(\ell_\pi\, I m_\pi\, I_z / JM)$$

$$\times\; Y^*_{\ell_p m_p}(\hat{p})\, Y_{\ell_\pi m_\pi}(\hat{K})\,\langle JM;\, \ell_\pi\, I(-)\,|\, H_I \,|\, JM;\, c\,(+)\rangle \; . \tag{3.13}$$

Then the formula for the differential cross section of (p, π^+)
reaction, on the target nucleus I_0 to the specific residual nuclear
state I, can be derived from eqs. (3.13) and (2.2) with the Racah
algebra as follows[*]:

$$\frac{d\sigma}{d\Omega} = \frac{\pi^2}{2}\, \frac{E_p}{p}\, k\, E_\pi\, \frac{1}{[I_0]}\, \sum_{\substack{\ell_p \ell_p' \ell_\pi \ell_\pi' L \\ J\, J'\, j_p\, j_p'}} i^{\,\ell_p - \ell_\pi}\, i^{\,\ell_\pi' - \ell_p'}\, (-)^{I - I_0 - \frac{1}{2}}$$

$$(-)^{j_p + j_p' + L}\, [J][J']\,\sqrt{[j_p][j_p'][\ell_p][\ell_p'][\ell_\pi][\ell_\pi']}$$

$$(\ell_p\, \ell_p'\, 0\, 0 / L\, 0)\, (\ell_\pi\, \ell_\pi'\, 0\, 0 / L\, 0)\, W(j_p\, \ell_p\, j_p'\, \ell_p';\, \tfrac{1}{2}\, L)$$

$$W(J\, \ell_\pi\, J'\, \ell_\pi';\, I L)\, W(J\, j_p\, J'\, j_p';\, I_0\, L)$$

$$\langle J;\, \ell_\pi\, I(-)\,\|\, H_I \,\|\, J;\, c\,(+)\rangle\,\langle J';\, \ell_\pi'\, I(-)\,\|\, H_I\,\|\, J';\, c'\,(+)\rangle^*$$

$$P_L(\cos\theta) \; . \tag{3.14}$$

---

[*] The reduced nuclear matrix element is defined for the tensor
operator Ξ_{JM} of rank J as $\langle j'm'|\, \Xi_{JM}\, |j\, m\rangle = (jJmM|j'm')\langle j'\|\, \Xi_J\, \|j\rangle$.

where

$$[J] = 2J + 1 , \quad etc.$$

Here p and E_p are the momentum and the total energy of the proton, respectively, and k and E_π are the same for the pion. P_L is the Legendre polynomial. In the case of the spin-zero target nucleus ($I_0 = 0$), eq. (3.14) is reduced to

$$\frac{d\sigma}{d\Omega} = \frac{\pi^2}{2} \frac{E_p}{p} k E_\pi \sum i^{\ell_p - \ell_\pi} i^{\ell_\pi' - \ell_p'} (-)^{I - \frac{1}{2}}$$

$$[j_p][j_p'] \sqrt{[\ell_p][\ell_p'][\ell_\pi][\ell_\pi']} (\ell_p \ell_p' 0 0 / L 0)(\ell_\pi \ell_\pi' 0 0 / L 0)$$

$$W(j_p \ell_p j_p' \ell_p'; \tfrac{1}{2} L) W(j_p \ell_\pi j_p' \ell_\pi'; I L)$$

$$\langle j_p; \ell_\pi I(-) \| H_I \| j_p; c(+) \rangle \langle j_p'; \ell_\pi' I(-) \| H_I \| j_p'; c'(+) \rangle^*$$

$$P_L(\cos\theta) . \tag{3.15}$$

Due to the property of the Racah coefficient, the following selection rules hold in eq. (3.15).

$$|\ell_p - \ell_p'| \leq L \leq \ell_p + \ell_p' \quad , \quad |\ell_\pi - \ell_\pi'| \leq L \leq \ell_\pi + \ell_\pi'$$

$$|j_p - j_p'| \leq L \leq j_p + j_p' \quad , \quad |j_p - \ell_\pi| \leq I \leq j_p + \ell_\pi . \tag{3.16}$$

The transition matrix element in eq. (3.14) can be explicitly written in the coordinate space,

$$\langle J; \ell_\pi I(-) \| H_I \| J; c(+) \rangle$$

$$= \sum_{I'} \sqrt{\frac{[I']}{[J]}} \langle \Phi_{I'} \| \sum_{s=1}^{A+1} B_s^{\ell_\pi I} \cdot \tau_s^{(-)} \| \Phi_c^{(+) J} \rangle \tag{3.17}$$

-15-

where

$$\Xi_s^{\eta\,\ell_\pi I} = -\sqrt{4\pi}\,\frac{f}{\mu}\,\frac{1}{\sqrt{E_\pi}}\,\sum_{\ell_\pi'}(-)^{\ell_\pi'}\,\sigma_s\,\nabla_s\,\psi_{\ell_\pi'I'}^{(-)\ell_\pi I*}(r_s)\,Y_{\ell_\pi'}^{*}(\hat{r}_s)\,, \qquad (3.18)$$

Here, $\psi_{\ell_\pi'\,I'}^{(-)\ell_\pi I}(r)$ is the radial wave function of the pion in the channel (ℓ_π', I'). The upper index (ℓ_π, I) represents the channel with the outgoing wave. $\tau^{(-)}$ is the isospin lowering operator for the nucleon. The initial wave function with total angular momentum J is denoted as $\Phi_c^{(+)J}$ and Φ_I is the wave function of the residual nucleus.

3.C. Correction to the nuclear recoil

In the (p,π^+) reaction, the recoil energy of the target nucleus is about 10 MeV for light nuclei. Therefore, the effect of the nuclear center of mass motion in the transition matrix element can not be neglected. To study this effect, we first separate the internal and the center of mass coordinates of the target and the residual nucleus explicitly, assuming the single particle model for the nucleus.

In the plane wave approximation, the transition amplitude M_{pw} is symbolically written as

$$M_{pw} \propto \langle \Psi_f | \sigma K \delta(x_p - x_\pi)\,e^{-iK(x_\pi - x_R')}\,e^{iP(x_p - x_R)} | \Psi_i \rangle, \qquad (3.19)$$

where ψ_i and ψ_f are the intrinsic wave functions of the target and the residual nucleus, respectively. The x_p and x_π are the coordinates of the proton and pion, and x_R and $x_{R'}$ are for the target and the residual nucleus, respectively (see Fig.2). Here, the coordinate $x_{R'}$ is expressed by the x_p and x_R as

$$x_R' = \frac{x_p + A x_R}{A + 1}, \qquad (3.20)$$

A being the mass number of the target. Then the matrix element M_{pw} can be written

$$M_{pw} \propto \langle \Psi_i | \phi_B(\mathbf{r}) \, \sigma \mathbf{K} \, e^{-i\mathbf{K}(\mathbf{x}_p - \frac{\mathbf{x}_p + A\mathbf{x}_R}{A+1})} e^{i\mathbf{P}\mathbf{r}} | \Psi_i \rangle$$

$$= \int \phi_B(\mathbf{r}) \, \sigma \mathbf{K} \, e^{-i\mathbf{K}\frac{A}{A+1}\mathbf{r}} e^{i\mathbf{P}\mathbf{r}} d\mathbf{r}$$

$$= \frac{A+1}{A} \int \phi_B(\mathbf{r}) \, \sigma \mathbf{K}' \, e^{-i\mathbf{K}'\mathbf{r}} e^{i\mathbf{P}\mathbf{r}} d\mathbf{r} \qquad (3.21)$$

where

$$\mathbf{r} = \mathbf{x}_p - \mathbf{x}_R \quad,$$

and

$$\mathbf{K}' = \frac{A}{A+1} \mathbf{K} \quad.$$

$\phi_B(\mathbf{r})$ is the single particle wave function of the transferred neutron. In deriving (3.21), we have assumed that the residual nucleus consists of the target nucleus plus one-neutron state. Thus, the inclusion of the nuclear recoil effect changes the pion momentum $\mathbf{K}$ in eq. (3.19) to $A\mathbf{k}/(A+1)$ and multiplies the transition matrix elements with a factor $(A+1)/A$.

Similarly the matrix element M_{DW} in the distorted wave approximation is given by

$$M_{DW} \propto \left(\frac{A+1}{A}\right)^2 \int \tilde{\phi}_B(\mathbf{P}'-\mathbf{K}') \, \sigma \mathbf{K}' \phi_\pi \left(\frac{A+1}{A} \mathbf{K}'\right) \phi_p(\mathbf{P}') d\mathbf{K}' d\mathbf{P}', \quad (3.22)$$

where $\tilde{\phi}_B$, ϕ_π and ϕ_p are the momentum-space wave functions of the

bound neutron, emitted pion and the incident proton, respectively.
The effect of the nuclear recoil is then easily taken into account by
modifying the pion momentum effectively. The numerical evaluation of
the nuclear recoil effect is given in section 6.

4. Optical potentials for proton and pion

As was discussed in section 2, the distortion of the pion and the proton wave functions is expected to give a significant change of the (p, π^+) cross section. In order to evaluate this effect, we first determine the optical potentials which represent the nuclear interactions with these particles.

4.A. Optical potential for proton

The experiment of the elastic scattering of the 180 MeV proton on light nuclei was performed by Johansson et al.[18,19]. They analysed their data by adopting the following optical potential phenomenologically,

$$V(r) = U f_1(r) + i W f_2(r)$$
$$+ \left(\frac{1}{\mu}\right)^2 \left[U_s \frac{d f_3(r)}{dr} + i W_s \frac{d f_4(r)}{dr} \right] \frac{1}{r} \ell \sigma . \qquad (4.1)$$

Here, μ is the pion mass, and ℓ and σ are the operators for the orbital angular momentum and spin of the proton, respectively. The Woods-Saxon type nuclear form factors $f_i(r)$ are adopted

$$f_i(r) = 1 \Big/ \left[1 + exp\left(\frac{r - R_i}{a_i}\right) \right] \qquad (4.2)$$

where a_i are diffusenesses and R_i the nuclear radii. Johansson et al. made a parameter search of the best fit with the data of 180 MeV elastic-scattering cross section and the polarization of the 173 and 155 MeV protons[20,21]. The parameters U, W, U_s, W_s, R_i and a_i for ^{12}C are listed in Table I.

4.B. Optical potential for pion

The optical potential for the pion is in principle derived from the multiple scattering theory with the data of the pion-nucleus scattering. We shortly review the derivation of the original pion-nucleus Kisslinger-potential[6,7,22-28]).

The pion-nucleus transition matrix $T_{\pi N}(E)$ is expressed in terms of the pion-nucleon scattering amplitude $t_{\pi N}$ and the Hamiltonian of the target nucleus H_N. The integral equation for the operator $T_{\pi N}(E)$ is

$$T_{\pi N}(E) = \sum_i v_i + \sum_i v_i \, G(E) \, T_{\pi N}(E) \, , \qquad (4.3)$$

where many-body Green function $G(E)$ is given by

$$G(E) = \frac{1}{E - K_\pi - H_N + i\varepsilon} \, . \qquad (4.4)$$

The v_i is the pion-nucleon potential and K_π the kinetic energy operator for the pion. The free pion-nucleon scattering amplitude $t_{\pi N}$ satisfies

$$t_{\pi N}(i) = v_i + v_i \, G_0(E) \, t_{\pi N}(i) \, , \qquad (4.5)$$

and

$$G_0(E) = \frac{1}{E - K_\pi - K_N + i\varepsilon} \, , \qquad (4.6)$$

where K_N is the kinetic energy operator of the nucleon.

Because the t-matrix is directly connected to the pion-nucleon

experimental data but not the potential v_i, we eliminate the pion-

nucleon potential v_i in eqs. (4.3) and (4.5). For this sake, we

introduce the " bound " collision matrix $\tau_i(E)$ as

$$\tau_i(E) = v_i + v_i \, G(E) \, \tau_i(E) \; . \qquad (4.7)$$

The operator $\tau_i(E)$ describes the scattering of the pion by the i-th

nucleon in the nucleus and is related to the free pion-nucleon scattering

matrix $t_{\pi N}$ as

$$\tau_i(E) = t_{\pi N}(i) + t_{\pi N}(i) \, (G(E) - G_0(\omega)) \, \tau_i(E) \; , \qquad (4.8)$$

where ω is the total energy in the pion-nucleon CM system. Then

the pion-nucleus scattering amplitude $T_{\pi N}(E)$ is expanded by the

" bound " collision matrix $\tau_i(E)$ as

$$T_{\pi N}(E) = \sum_i \tau_i + \sum_{i \neq j} \tau_i \, G(E) \, \tau_j + \sum_{\substack{i \neq j \\ j \neq k}} \tau_i \, G(E) \, \tau_j \, G(E) \, \tau_k + \cdots \qquad (4.9)$$

The eq. (4.9) has a simple physical meaning. The first term represents

the pion-nucleon scattering in the nucleus and the following terms

represent the multiple scattering series of the pion in the nuclear

medium. Thus the pion-nucleus scattering matrix $T_{\pi N}(E)$ is formally

related to the free pion-nucleon transition matrix $t_{\pi N}$. It is hard,

however, to use eqs. (4.8) and (4.9) without any approximation in the

actual calculations, because of the complexity of the many-body

Green function G(E) involved. In order to study the elastic scattering of the pion, we define the pion optical potential V_π as,

$$\langle 0|T_{\pi N}(E)|0\rangle = V_\pi + V_\pi \langle 0|G(E)|0\rangle\langle 0|T_{\pi N}(E)|0\rangle, \qquad (4.10)$$

where $|0\rangle$ stands for the nuclear ground state, and optical potential V_π is the function of the pion coordinate only. Once the optical potential V_π is known, it is sufficient for us to solve the one body Klein-Gordon equation and the exact answer of the elastic scattering can be obtained. To obtain the optical potential V_π we make the following two approximations.

(i) Coherent approximation

In the multiple scattering series (4.9), we take only the ground state for the intermediate states,

$$\langle 0|T_{\pi N}|0\rangle = \langle 0|\sum_i \tau_i|0\rangle + \sum_{i \neq j} \langle 0|\tau_i|0\rangle\langle 0|G(E)|0\rangle\langle 0|\tau_j|0\rangle + \cdots$$

$$= A\langle 0|\tau_1|0\rangle + A\langle 0|\tau_1|0\rangle\langle 0|G(E)|0\rangle\left(\frac{A-1}{A}\langle 0|T_{\pi N}|0\rangle\right)$$

$$(4.11)$$

and eq. (4.11) can be rewritten as,

$$\frac{A-1}{A}\langle 0|T_{\pi N}|0\rangle = (A-1)\langle 0|\tau_1|0\rangle$$

$$+ (A-1)\langle 0|\tau_1|0\rangle\langle 0|G(E)|0\rangle\left(\frac{A-1}{A}\langle 0|T_{\pi N}|0\rangle\right).$$

$$(4.12)$$

The factor A in eq. (4.11) is a consequence of the antisymmetrization of the nuclear wave function. Then the optical potential V_π is given by

$$V_\pi = (A-1) \langle o | \tau_1 | o \rangle \qquad\qquad (4.13)$$

(ii) Impulse approximation

We neglect the binding effects for nucleons. The " bound " collision matrix τ_i is replaced approximately by free pion-nucleon t-matrix $t_{\pi N}$. The optical potential is then given by,

$$V_\pi = (A-1) \langle o | t_{\pi N} | o \rangle \qquad\qquad (4.14)$$

Under these assumptions, the optical potential is determined by the gross properties of the nucleus, like density, and is independent on the detailed dynamics of the target nucleus. The optical potential under the above two assumptions can explicitly be written as

$$\langle K' | V_\pi | K \rangle = (A-1) \sum_{\substack{m_\tau, m_s \\ m_c', m_s'}} \int dP dP' \langle K' m_I'; P' m_s' m_c' | t_{\pi N} | K m_I; P m_s m_c \rangle$$
$$\times F(P' m_s' m_c'; P m_s m_c) \qquad\qquad (4.15)$$

where

$$F(P' m_s' m_c'; P m_s m_c) = \sum_{\substack{m_{s_2} \cdots m_{s_A} \\ m_{c_2} \cdots m_{c_A}}} \int dP_2 \cdots dP_A \; \Psi_0^*(P' m_s' m_c'; P_2 m_{s_2} m_{c_2}, \cdots; P_A m_{s_A} m_{c_A})$$
$$\times \Psi_0(P m_s m_c, P_2 m_{s_2} m_{c_2}, \cdots; P_A m_{s_A} m_{c_A}) \qquad\qquad (4.16)$$

Here Ψ_0 is the ground-state wave function of the target nucleus, m_s is the spin projection of the nucleon, and m_τ and m_I are the isospin projection of the nucleon and the pion, respectively.
The eq. (4.15) is further simplified by factorizing out the $t_{\pi N}$-matrix at the some averaged nucleon momentum p_0. Considering the momentum conserving delta function in the $t_{\pi N}$-matrix

$$\langle K' | V_\pi | K \rangle = \sum \langle K' m_I', P_0 - g \; m_s' m_c' | t_{\pi N} | K m_I, P_0 m_s m_c \rangle$$
$$\times \rho_{m_s' m_c'; m_s m_c}(g) \qquad\qquad (4.17)$$

where

$$\rho_{m_s' m_t'; m_s m_t}(q) = \int F(P-q\, m_s' m_t'\, ; P\, m_s\, m_t)\, dP \qquad (4./8)$$

and

$$q = K' - K \; .$$

For the nucleus of the spin zero, and for the positive pion, the eq. (4.17) simplifies to

$$\langle K' | V_\pi | K \rangle = \langle K', P_0 - q\, m_t | t_1 | K, P_0 m_t \rangle\, \rho(q) \cdot (2\pi)^3 \qquad (4./9)$$

and

$$\rho(q) = (2\pi)^{-3} \sum_{m_t} \int e^{i q \cdot r} \widetilde{\rho}_{m_t}(r)\, dr$$

where t_1 is the spin-nonflip part of the pion-nucleon t-matrix and $\widetilde{\rho}_{m_t}(r)$ is the nucleon-density function. In eq. (4.19) the t_1-matrix represents the power of the pion-nucleon scattering and $\rho(q)$ the probability of the nucleus to remain in the ground state after the collision. The spin non-flip part of the pion-nucleon t-matrix can generally be expressed in the pion-nucleon CM system as[22]),

$$\langle K' | t_1(\omega) | K \rangle = \frac{1}{4\pi} \sum_\ell \left[\left\{ (\ell+1) \frac{2t_{\ell+}^{3/2} + t_{\ell+}^{1/2}}{3} + \ell \frac{2t_{\ell-}^{3/2} + t_{\ell-}^{1/2}}{3} \right\} \right.$$
$$\left. + \left\{ (\ell+1) \frac{t_{\ell+}^{3/2} - t_{\ell+}^{1/2}}{3} + \ell \frac{t_{\ell-}^{3/2} - t_{\ell-}^{1/2}}{3} \right\} \tau T \right] P_\ell(\cos\theta) , \qquad (4.2/)$$

where K and ω are the momentum of the pion, and the total energy of the pion and the nucleon in the pion-nucleon CM system. T and τ are the pion and the nucleon isospin operators. The symbol $\ell\pm$ represents the total angular momentum $j = \ell\pm 1/2$ and the superscript of $t_{\ell\pm}$ represents the isospin of the pion-nucleon eigenchannel. The t-matrix in eq. (4.21) is related to the pion-nucleon scattering phase shifts by

$$t'_{\ell t} = -\frac{1}{\pi}\frac{1}{\kappa}\frac{E_\pi(\kappa)+E_n(\kappa)}{E_\pi(\kappa)E_n(\kappa)}e^{i\delta_{\ell t}}\sin\delta_{\ell t'} \qquad (4.22)$$

where

$$E_\pi(\kappa) = \sqrt{\kappa^2+\mu^2} \quad,$$

and $\qquad\qquad\qquad\qquad\qquad\qquad\qquad\qquad\qquad (4.23)$

$$E_n(\kappa) = \sqrt{\kappa^2+m_p^2} \quad.$$

In order to calculate the optical potential by the phase shifts,

it is necessary to transform the t-matrix in the pion-nucleon CM

system to the one in the pion-nucleus CM system. Assuming the nucleon

at rest in the pion-nucleus CM system ($p_0 = 0$), we have

$$\langle k'| t_{\ell t}(E)|k\rangle = \gamma\langle \kappa'|t_{\ell t}(\omega)|\kappa\rangle \quad, \qquad (4.24)$$

where

$$\gamma = \sqrt{\frac{E_\pi(\kappa)\,E_\pi(\kappa')\,E_n(\kappa)\,E_n(\kappa')}{E_\pi(k)\,E_\pi(k')\,E_n(0)\,E_n(0)}} \;\simeq\; \frac{E_\pi(\kappa)E_n(\kappa)}{E_\pi(k)\,m_p} \qquad (4.25)$$

In the low energy region that we are concerned, the s and p-wave

interactions dominate. Retaining only the s and p-wave parts in eq.

(4.21), we finally obtain the pion optical potential of the form,

$$2E_\pi\langle k'|V_\pi(E_\pi)|k\rangle = -b_0\,k_0^2\,\rho(q) + b_1\,\rho(q)\,k k' \qquad (4.26)$$

where

$$\rho(q) = (2\pi)^{-3}\int e^{iqr}\widetilde{\rho}(r)\,dr \qquad (4.27)$$

and

$$E_\pi = \sqrt{k_0^2+\mu^2} \quad.$$

Here, $\widetilde{\rho}(r)$ is the nuclear density, normalized to the nucleon number A.

The potential parameters b_0 and b_1 are given by the pion-nucleon phase

shifts as,

$$b_0 = \frac{4\pi}{k_0\kappa^2}\frac{1}{A}\left[\frac{N}{3}(\alpha_3+2\alpha_1)+(A-N)\alpha_3\right] \;, \quad (\alpha_{2T}) \qquad (4.28)$$

$$b_1 = \frac{4\pi}{k_0 \chi^2} \frac{1}{A} \left[\frac{N}{3} (2\alpha_{33} + \alpha_{31} + 4\alpha_{13} + 2\alpha_{11}) \right.$$
$$\left. + (A-N)(2\alpha_{33} + \alpha_{31}) \right] , \qquad (\alpha_{2T, 2J}) \qquad (4.29)$$

where $\alpha_i = e^{i\delta_i} \sin\delta_i$, and N is the neutron number of the target nucleus.

In deriving the eq. (4.26) we have implicitly assumed that the off-shell extrapolation of the p-wave interaction is of the form $\mathbb{K}\mathbb{K}'$ and have neglected the possible effects of the scattering angle transformation between the pion-nucleon and the pion-nucleus CM system.[15,29])

This potential (4.26), originally derived by Kisslinger[7]), is widely applied to the analysis of the pion-nucleus elastic scattering.

Usually, the parameters b_0 and b_1 in eq. (4.26) are treated as free parameters. Only the parametrization of the type (4.26) is assumed.

Several authors have analysed the data of elastic scattering by adopting the potential (4.26) and assuming the b_0 and b_1 as free parameters, and obtained the best fit parameters b_0 and b_1 for the available data. The best fit values for the low energy $\pi^+ - {}^{12}C$ elastic scattering by Auerbach et al.[28]), Marshall et al.[30]) and Amann et al.[31]), are shown in Figs. 3 and 4 with the theoretical values predicted by eqs. (4.28) and (4.29). The pion-nucleon phase shifts are taken from the work of Roper et al.[32]). In general, the best fit parameters are not so different from the theoretical parameters. But $\text{Re} b_0$ is an exception. Especially, at low energy ($T_\pi \lesssim 60$ MeV), the discrepancies between the best fit and the theoretical values are remarkable.

Energy dependences of the parameters b_0 and b_1 are qualitatively understood by the low-energy behavior of the phase shifts $\delta_\ell \sim k^{2\ell+1}$.

$$\text{Re} b_0 \sim 1/k^2$$

$$\text{Im} b_0 \sim 1/k$$

$$\text{Re} b_1 \sim \text{constant} \qquad\qquad (4.30)$$

$$\text{Im} b_1 \sim k^3$$

In fact, the calculated values by pion-nucleon phase shifts in Figs.

3 and 4 show the energy dependences in eq. (4.30), except Reb_0.

The unexpected behavior of the Reb_0 is the consequence that the low-

energy s-wave pion-nucleon interaction is dominated by the isovector

type and the isoscalar interaction is very small. Therefore the Reb_0

for the isospin-zero nucleus is almost cancelled and then the multiple

scattering or the in medium corrections might be important. These are

considered to be the reason for the discrepancies seen in Reb_0 of Fig.3.

This will be discussed in detail in section 6.

The Kisslinger-potential in eq. (4.26) has the following non-local

character in the coordinate space.

$$2E_\pi V_\pi(r) = -b_0 k_0^2 \tilde{\rho}(r) + b_1 \nabla \tilde{\rho}(r) \nabla \qquad (4.31)$$

The Klein-Gordon equation for the radial wave function for ℓ-th partial

wave is then[33])

$$\left[\frac{d^2}{dr^2} + \left(\frac{2}{r} - \frac{b_1}{1-b_1\tilde{\rho}(r)}\frac{d}{dr}\tilde{\rho}(r)\right)\frac{d}{dr} - \frac{\ell(\ell+1)}{r^2} + \frac{k_0^2 + b_0 k_0^2 \tilde{\rho}(r) - 2E_\pi V_c}{1 - b_1 \tilde{\rho}(r)}\right]\psi_\ell = 0. \quad (4.32)$$

Here V_c is the Coulomb potential. For the nuclear density $\tilde{\rho}(r)$, we

adopt the following form for ^{12}C,

$$\tilde{\rho}(r) = \frac{24}{\pi^{3/2}[2+3w]b^3}[1 + w(\frac{r}{b})^2] e^{-(\frac{r}{b})^2}. \qquad (4.33)$$

In the harmonic oscillator model $w = 4/3$ and the b is determined

by the experiment of the electron scattering as $b = 1.64$ fm for ^{12}C[34,35]).

In order to see the effects of the interior of the nuclear density,

we choose the parameters $w = 1$ and $b = 1.72$ fm, which simulate the

Fermi-type density distribution. The $\tilde{\rho}(r)$ is shown in Fig.5.

So far we have assumed the off-shell extrapolation for the p-wave

part of the Kisslinger-potential to be the form $\vec{k}\vec{k}'$. Since the factor

$|K|K'$ is divergent far off the energy shell ($|\mathbb{k}| \neq |\mathbb{k}'|$), it may be an overestimation of the off-shell interaction. The elastic scattering is , however, not so sensitive to the off-shell behavior of the pion optical potential. And this is the reason why the parametrization of the original Kisslinger-potential succeeded in the analysis of the pion elastic scattering. On the other hand, the off-shell part in the pion optical potential is expected to be substantially important for the (p, π^+) reaction. (See the discussion in section 2.) For these reasons, we make a modification for eq. (4.26) as follows :

$$2E_\pi \langle K'|V_\pi(E_\pi)|K\rangle = -b_0 \, k_0^2 \, P(q) + b_1 P(q) \, g(K) \, K \cdot K' g(K') \qquad (4.34)$$

Here, g(k) is the pion-nucleon vertex function, which is analogous to the nucleon form factor in the Chew-Low theory, and improves the off-shell behavior of the p-wave part optical potential. It is normalized to one, on the energy shell,

$$g(K_0) = 1 \qquad\qquad (4.35)$$

Phenomenologically we have adopted the Gaussian-type for the vertex function

$$g(K) = e^{\frac{k_0^2 - k^2}{\Lambda^2}} \qquad\qquad (4.36)$$

where Λ is the cut- off mass.

We have calculated the pion elastic-scattering cross section on ^{12}C by the potential (4.34) to see the cut-off mass or the nuclear form-factor dependences. The parameters b_0 and b_1 are shown in Table II. The Set I is the best fit value to the 30.2 MeV pion elastic scattering on ^{12}C[30)], and Set II is the theoretical value calculated by the pion-nucleon phase shifts using the eqs. (4.28) and (4.29). The results are shown in Fig.6. The curve a is the calculated cross section for 34.3 MeV

elastic scattering with Coulomb interaction. The experimental values

for 30.2 MeV are by Marshall et al.[30]), and for 31.5 MeV by Kane[36]).

When the cut-off function g(k) is employed, it is necessary to solve

the Klein-Gordon equation in momentum space and then we have neglected

the Coulomb force. The curves b and c (d and e) show the calculated

cross section without the Coulomb interaction for several cut-off masses

and the nuclear form factor w = 4/3 and b = 1.64 (w = 1 and b = 1.72).

Since the Coulomb interaction is neglected, the results can not be

directly compared with the experimental data, but we can see immediately

that the cut-off mass or the nuclear form factor dependences are very

small or even negligible. Therefore the off-shell behavior of the

pion potential is difficult to study from the elastic scattering.

In other words, the optical potential (4.34) is still ambiguous in the

off-shell part. For comparison, we have shown in Fig. 6, the calculated

cross section by the potential Set II (curve f). The failure of this

first-order potential is obvious.

5. Distorted waves of proton and pion

In order to evaluate the (p, π^+) reaction cross section with the formalism in section 3, we have to obtain the distorted waves of the incident proton and the emitted pion. In this section we describe the numerical methods to obtain the distorted waves.

5.A. Distorted wave of proton

The distorted wave of the proton is obtained by solving the Schrödinger equation numerically. The differential equation for the radial part $u_\ell(r)/r$ of the ℓ-th partial wave is

$$\left\{ \frac{1}{2m_p}\left[-\frac{d^2}{dr^2} + \frac{\ell(\ell+1)}{r^2} \right] + V_p(r) - T_p \right\} u_\ell(r) = 0 \quad . \tag{5.1}$$

Here m_p and T_p are the mass and kinetic energy of the proton, respectively, and $V_p(r)$ is the proton optical potential given in section 4. We solve eq. (5.1) under the outgoing-wave boundary condition, where the asymptotic form of $u_\ell^{(+)}(r)$ is given by,

$$u_\ell^{(+)}(r) \xrightarrow[r \longrightarrow \infty]{} \sqrt{\frac{2}{\pi}} \frac{1}{p} \, e^{i\delta_\ell} \sin\left(pr + \delta_\ell - \frac{\ell\pi}{2} \right) \, . \tag{5.2}$$

Here δ_ℓ is the phase shift of the ℓ-th partial wave. In the calculation of the (p, π^+) reaction cross section, the Coulomb interaction is neglected because the energy of the incident proton is high enough. We adopt the standard Runge-Kutta method with 720 points to solve the eq. (5.1) numerically.

5.B. Distorted wave of pion

The numerical procedure to obtain the pion distorted wave function in the coordinate space is almost the same as that for the proton wave function. The Klein-Gordon equation in the coordinate space is given by

$$(-\nabla^2 + \mu^2 - E_\pi^2)\, \psi_{K_0}(r) = -2 E_\pi V_\pi\, \psi_{K_0}(r) \quad . \qquad (5.3)$$

If the original Kisslinger-type optical potential or the local potential is applied, the eq. (5.3) is nothing but a ordinary differential equation. But as was mentioned in section 4, the optical potential V_π that we are going to study is far from the local one and it is necessary to solve the eq. (5.3) in the momentum space. We define the pion wave function in the momentum space as

$$\phi_{K_0}(K) = (2\pi)^{-3/2} \int e^{-iK\cdot r}\, \psi_{K_0}(r)\, dr \quad , \qquad (5.4)$$

The wave function $\phi_{K_0}(K)$ satisfies the following integral equation.

$$(K^2 - K_0^2)\, \phi_{K_0}(K) = -2E_\pi \int \langle K | V_\pi | K' \rangle\, \phi_{K_0}(K')\, dK' \quad . \qquad (5.5)$$

The normalization of the wave function is chosen to be the momentum delta function as,

$$\int \phi_{K_0}^*(K)\, \phi_{K_0'}(K)\, dK = \delta(K_0 - K_0') \quad . \qquad (5.6)$$

To reduce the number of variables, we perform the multipole expansion

of the wave function and the optical potential as follows.

$$\phi_{K_0}(\mathbb{K}) = \sum_{\ell m} \phi_\ell^{K_0}(K) Y_{\ell m}^*(\hat{\mathbb{K}}_0) Y_{\ell m}(\hat{\mathbb{K}}) ,\qquad (5.7)$$

$$\psi_{K_0}(\mathbb{r}) = \sum_{\ell m} i^\ell \psi_\ell^{K_0}(r) Y_{\ell m}^*(\hat{\mathbb{K}}_0) Y_{\ell m}(\hat{\mathbb{r}}) ,\qquad (5.8)$$

$$\langle \mathbb{K} | V_{\pi} | \mathbb{K}' \rangle = \sum_{\ell m} \langle K | V^\ell | K' \rangle Y_{\ell m}(\hat{\mathbb{K}}) Y_{\ell m}^*(\hat{\mathbb{K}}') .\qquad (5.9)$$

The radial wave fuctions $\psi_\ell^{K_0}(r)$ in the coordinate space and $\phi_\ell^{K_0}(k)$

in the momentum space are related to each other by the integral

transformation as

$$\psi_\ell^{k_0}(r) = \sqrt{\frac{2}{\pi}} \int_0^\infty j_\ell(kr)\, \phi_\ell^{k_0}(k)\, k^2 dk ,\qquad (5.10)$$

where $j_\ell(kr)$ is the spherical Bessel function. The original equation

(5.5) is reduced to the integral equation in one variable.

$$(k^2 - k_0^2)\, \phi_\ell^{k_0}(k) = -2E_\pi \int_0^\infty \langle k | V^\ell | k' \rangle \phi_\ell^{k_0}(k') k'^2 dk' \qquad (5.11)$$

The equation (5.11) can be solved numerically in an analogous way

as in the continuum shell model calculations[37]. The solution of the

eq. (5.11) has the singularity on the energy shell ($k = k_0$) and

its general form is given by,

$$\phi_\ell^{k_0}(k) = \frac{2}{k_0} \left[A\, \delta(k^2 - k_0^2) + P\, \frac{B(k)}{k^2 - k_0^2} \right] .\qquad (5.12)$$

For convinience, we have chosen the principal part of the integral

for the second term of the above equation. The structure of the

singularity in eq. (5.12) determines the asymptotic behavior of the

wave function in the coordinate space. In fact, it is given by,

$$\psi_\ell^{k_0}(r) \xrightarrow[r \to \infty]{} - \frac{1}{2 i k_0 r} \sqrt{\frac{2}{\pi}} \left[(A - i\pi B(k_0)) e^{-i(k_0 r - \frac{\ell\pi}{2})} \right.$$

$$\left. - (A + i\pi B(k_0)) e^{i(k_0 r - \frac{\ell\pi}{2})} \right] . \qquad (5.13)$$

Substituting eq. (5.12) into eq. (5.11) we have

$$- B(k) = E_\pi \langle k | V^\ell | k_0 \rangle \cdot A k_0$$

$$+ 2 E_\pi \int_0^\infty \frac{P}{k'^2 - k_0^2} \langle k | V^\ell | k' \rangle B(k') k'^2 dk' . \qquad (5.14)$$

This is numerically solved by replacing the integral to the discrete

sum. The eq. (5.14), then, reduces to the algebraic equation.

To carry out this procedure, the principal part of the integral in

eq. (5.14) must be handled carefully. In general, the principal

part of the integral

$$I = P \int_0^{k_{max}} \frac{a(k')}{k' - k_0} dk' \qquad (5.15)$$

can be separated into two terms. (a(k) is the arbitrary function

without singularity.)

$$I = \int_0^{k_{max}} \frac{a(k') - a(k_0)}{k' - k_0} dk' + P \int_0^{k_{max}} \frac{a(k_0)}{k' - k_0} dk' \qquad (5.16)$$

For the first term of which the integrand has no singularity, the standard method of the numerical integration can be applied. The principal part in the second integral can be easily performed and we obtain,

$$I = \sum_i \alpha_i \; \frac{a(k_i) - a(k_0)}{k_i - k_0} + a(k_0) \; \ell n \; \frac{k_{max} - k_0}{k_0} \qquad (5.17)$$

$$= \sum_i \alpha_i \; \frac{a(k_i)}{k_i - k_0} + C \cdot a(k_0) \qquad (5.18)$$

where

$$C = \ell n \left(\frac{k_{max} - k_0}{k_0} \right) - \sum_i \frac{\alpha_i}{k_i - k_0} \qquad (5.19)$$

The weighting factor for the i-th point in the numerical integration is denoted as α_i. The eq. (5.14) is written as

$$-B(k) = E_\pi k_0 \left[A + C \, B(k_0) \right] \langle k | V^\ell | k_0 \rangle$$
$$+ 2 E_\pi \sum_j \frac{\alpha_j'}{k_j^2 - k_0^2} \langle k | V^\ell | k_j \rangle B(k_j) k_j^2 \qquad (5.20)$$

The variable k is also evaluated at each mesh point and we obtain the coupled equation for $B(k_i)$ and A,

$$-B(k_0) = E_\pi k_0 V_{00} X + 2 E_\pi \sum_j V_{0j} \frac{\alpha_j'}{k_j^2 - k_0^2} k_j^2 B(k_j) \qquad (5.21)$$

$$-B(k_i) = E_\pi k_0 V_{i0} X + 2 E_\pi \sum_j V_{ij} \frac{\alpha_j'}{k_j^2 - k_0^2} k_j^2 B(k_j) \qquad (5.22)$$

where

$$X = A + C \cdot B(k_0) , \qquad (5.23)$$

and

$$V_{0i} = \langle k_0 | V^\ell | k_i \rangle , \; etc. \qquad (5.24)$$

Finally, the algebraic equation that we must solve is given in the matrix representation :

$$\begin{bmatrix} V_{ij} + \dfrac{k_j^2 - k_0^2}{2E_\pi \alpha_j k_j^2} \delta_{ij} & \vdots & V_{i0} \\ & \vdots & \\ \hline V_{0j} & \vdots & V_{00} \end{bmatrix} \begin{pmatrix} 2E_\pi \dfrac{\alpha_j k_j^2}{k_j^2 - k_0^2} B(k_j) \\ \\ E_\pi k_0 [A + c\, B(k_0)] \end{pmatrix} = \begin{pmatrix} 0 \\ \hline -B(k_0) \end{pmatrix} \qquad (5.25)$$

In the eq. (5.25), the $B(k_0)$ is still undetermined and must be chosen so as to satisfy the required boundary conditions. For the outgoing-wave boundary conditions, we have

$$A - i\pi B(k_0) = 1 \quad . \qquad (5.26)$$

From eqs. (5.25) and (5.26), the pion wave function in the momentum space can be completely determined. The phase shift δ_ℓ , for example, can be obtained by

$$\delta_\ell = \frac{1}{2i} \ell n \left(A + i\pi B(k_0) \right) \qquad (5.27)$$

In practice we have adopted the Simpson's method of integration with the upper limit of the integral k_{max} = 1 GeV and the 60 mesh points. The calculated elastic-scattering cross sections are compared to the results by the coordinate-space calculations and the agreement is quite well.

To perform the above calculations, we need an explicit form for the pion optical potential of each ℓ-th wave. The optical potential given in section 4 is

$$2E_\pi \langle k' | V_\pi | k \rangle = -b_0 k_0^2 \rho(q) + b_1 \rho(q)\, j(k)\, k k' \, j(k') \; , \qquad (5.28)$$

where

$$\rho(q) = (2\pi)^{-3} \int d^3r \, e^{iq \cdot r} \tilde{\rho}(r) \qquad (5.29)$$

The nuclear density adopted there for ^{12}C is,

$$\tilde{\rho}(r) = \frac{24}{\pi^{3/2}[2+3w]b^3} \left[1 + w\left(\frac{r}{b}\right)^2\right] e^{-\left(\frac{r}{b}\right)^2} . \qquad (5.30)$$

The nuclear form factor $\rho(q)$ is then given by,

$$\rho(q) = \frac{3}{\pi^3[2+3w]} \left[\left\{1 + \frac{3}{2}w - \frac{1}{4}wb^2(k^2+k'^2)\right\} \right.$$
$$\left. + \frac{w}{2}b^2 kk'\right] e^{-\frac{b^2}{4}|k-k'|^2} . \qquad (5.31)$$

Using the equation

$$e^{-\frac{b^2}{4}|k-k'|^2} = e^{-\frac{b^2}{4}(k^2+k'^2)} e^{\frac{b^2}{2}kk'}$$

$$= e^{-\frac{b^2}{4}(k^2+k'^2)} \sum_{\ell=0}^{\infty} (2\ell+1) i_\ell\left(\frac{b^2}{2}kk'\right) P_\ell(\cos\theta) , \qquad (5.32)$$

we can perform the partial wave decomposition of the pion optical potential. Here, the $i_\ell(b^2 kk'/2)$ is the modified spherical Bessel function. For the ℓ-th multipole, we obtain

$$2E_\pi \langle k|V^\ell|k'\rangle = \frac{6}{\pi^2[2+3w]} e^{-\frac{b^2}{4}(k^2+k'^2)}$$

$$\times \left[-b_0 k_0^2 \left\{ (2+3w - \frac{w}{2}b^2(k^2+k'^2)) i_\ell(y) + wb^2 kk' i'_\ell(y) \right\} \right.$$

$$\left. - b_1 g(k) g(k') \left\{ (2+3w - \frac{w}{2}b^2(k^2+k'^2)) kk' i'_\ell(y) + wb^2(kk')^2 i''_\ell(y) \right\} \right] \qquad (5.33)$$

where

$$y = \frac{1}{2}b^2 kk' . \qquad (5.34)$$

When k or k' becomes large, the potential behaves as (without the cut-off factor g(k))

$$b^2 k \cdot k' e^{-\frac{b^2}{4}(k^2+k'^2)} i_\ell\left(\frac{b^2 kk'}{2}\right) \xrightarrow[k, k' \to \infty]{} e^{-\frac{b^2}{4}(k-k')^2} . \qquad (5.35)$$

In the domain $k \not\sim k'$ the interaction rapidly falls off, while $k \sim k'$ the interaction do not damp even when k and k' are very large.

But this does not cause any trouble in the numerical calculation, because the area where $k \sim k'$ is very small in the whole domain of the momentum space.

6. Results and discussions

In this section, we give the results of the numerical calculations of the $^{12}C(p, \pi^+)^{13}C$ reaction cross section in the distorted wave approximation. The pion and the proton distorted waves are calculated by the methods described in section 5. For the low-lying states of ^{13}C, the neutron can be transferred to one specific single particle orbit. The component of the residual nucleus with target nucleus plus one neutron, contributes to the transition matrix element. In the distorted wave approximation, therefore, the spectroscopic factor and the single particle wave function are the model-dependent quantities.

For the single particle wave function of the transferred neutron, we adopt the harmonic-oscillator type or the solution in the Woods-Saxon potential. For the Woods-Saxon potential, the strength of the spin-orbit force $U_{so} = 6MeV$, diffuseness $a = 0.65fm$ and the nuclear radius $R = 2.75fm$ are fixed, and the depth of the central potential is adjusted to reproduce the experimental single particle energies. Using the formula (3.15) in section 3, we have calculated the (p, π^+) reaction cross section. Because the energy of the emitted pion is low ($\sim 35MeV$), the contributions from the high partial wave can be neglected. We have taken into account the partial waves up to $\ell = 7$ for pion and all the proton partial waves that are allowed by the angular-momentum selection rule. The convergence of the calculated cross section is numerically checked.

First of all we have investigated the effect of the Coulomb interaction in (p, π^+) reaction cross section in the coordinate-space calculation because we neglect it in the momentum space. The curves a and b in Fig. 7 show the calculated cross section for $^{12}C(p, \pi^+)^{13}C$(ground state)

reaction with and without the Coulomb interaction. Here the parameters

for the pion optical potential Set I in Table II are employed. As is

seen there, the repulsive Coulomb force reduces the (p, π^+) reaction

cross section slightly in the forward direction, but is not so important

in the present analysis. Next, the effects of the proton distorted wave

are shown in Fig. .8. The curves a and b are the calculated cross section

for $^{12}C(p, \pi^+)^{13}C(3.09MeV;1/2^+)$ reaction with and without the distortion

of the proton wave. The effect of the proton distorted wave is to reduce

the absolute value of the cross section about an order of magnitude, but

the dependence to the potential parameters is expected to be small.

We have, therefore, fixed the parameters of the proton optical potential.

In order to see the effects of the pion distorted wave on (p, π^+)

reaction, we have calculated the $^{12}C(p, \pi^+)^{13}C$(ground state) reaction

cross section by the pion optical potential (4.34) with the parameters

Set I in Table II. At first, we investigate the cut-off mass Λ-dependence

of the cross section. In Fig.9, the curves a, b and c show the results

with the cut-off masses $\Lambda = \infty$, 1GeV and 700MeV, respectively. By the off-

shell cut-off factor $g(k)$, the cross section drastically reduces, and

it is in contrast to the results of the elastic scattering. The importance

of the effects of the pion optical potential, especially the off-shell

part , is obvious from these results. So far, we have assumed that the

pion nucleon vertex is described by the coupling constant f. Because

the emission of the off-shell pion is important in the (p, π^+) reaction,

we have cnnsidered the pion-nucleon vertex function $v(k^2)$ which is

normalized to one, on the energy shell,

$$v(k_0^2) = 1 \qquad\qquad (6.1)$$

and we have taken into account the vertex correction by replacing the

pion-nucleon coupling constant f as

$$f \longrightarrow f \cdot v(\kappa^2) \ . \tag{6.2}$$

Phenomenologically we have the Gaussian-type for $v(k^2)$

$$v(\kappa^2) = e^{\frac{k_0^2 - k^2}{\Lambda_v^2}} \tag{6.3}$$

where the cut-off mass Λ_v is assumed to be 700MeV. The curves d and e

in Fig. 9 are the results with nuclear recoil and the recoil plus vertex

corrections, respectively. (The nuclear recoil correction was discussed

in section 3.) As is seen there, these corrections reduce the cross

section about the factor 3, and are non-negligible. The curve f in the

same figure is the result by the first-order potential Set II. The

absolute value is about three order of magnitudes larger than the

experimental data. The failure of the first-order potential is obvious.

In order to see the importance of the off-shell part of the optical

potential in more detail, we have shown in Figs.10 and 11, the absolute

value of the pion optical potential $\left| \text{Re} \langle k' | v^{\ell}(E_{\pi}(k_0)) | k \rangle / k \right|$ for $\ell = 0$

and 1, and $k' = k_0 = 100$MeV ($E(k_0) = \sqrt{k_0^2 + \mu^2}$). Here, the parameters

Set I are adopted, and the cut-off mass Λ-dependences are shown.

As is seen there, the cut-off procedure greatly reduces the off-shell

interaction, especially far off the energy shell. In order to see the

off-shell effects on the pion wave function we have shown in Figs. 12

and 13, the real part of the pion wave function in momentum space, $\text{Re}\phi_{\ell}^{k_0}(k)$,

for $\ell = 0$ and 1, respectively. The curves a and b are the results with

off-shell cut-off masses $\Lambda = \infty$ and 700MeV, respectively. From these

figures we can understand that the strong cut-off mass Λ-dependence

of the (p, π^+) reaction cross section is due to the behavior of the

high-momentum parts of the pion wave function. It should be noticed

that the pion wave function neighbouring on the energy shell is scarcely

affected by the off-shell cut-off procedure, namely the elastic-scattering

cross section is insensitive to the off-shell part of the potential.

As to the first-order optical potential, the pion wave function c by

potential Set II, in Figs. 12 and 13, has a very large high-momentum

component which greatly enhances the (p, π^+) reaction cross section.

This is due to the strong p-wave nature of the potential Set II.

This property of the first-order optical potential is also seen in the

coordinate space wave function. Figs.14 and 15 show the pion wave

function in coordinate space, for $\ell = 0$ and 1, respectively. The curves

A and B are the results with the potential Set I and II, respectively.

The p-wave dominance of the potential Set II is reflected to the

behavior of the wave function B, especially around the nuclear radius.

The best-fit potential to the elastic scattering (Set I) is more close

to the local potential, because of the large local s-wave term.

Thus, the absolute value of the (p, π^+) reaction cross section

can be understood by the off-shell cut-off procedure in the Kisslinger-

potential. The angular distribution, however, is not well explained.

Because of the high-momentum transfer in the (p, π^+) reaction, the

interior of the nuclear density distribution will be important. In the

modified Kisslinger-potential (4.34), we use the nuclear density (4.33)

with w = 1 and b = 1.72 which differ from the harmonic-oscillator model

mainly interior of the nucleus (see Fig.5). The calculated cross section

with the single particle wave function in the Woods-Saxon potential is

shown in Fig.16. The curves a and b show the results with cut-off masses

Λ = 1.5GeV and 700MeV, respectively. They are in a good agreement

with the experimental data. Here, the vertex and the nuclear recoil

corrections are included. The curve c by the first-order potential

(Set II) is evidently against the data.

Our calculations show that the absolute value of the reaction cross section in $^{12}C(p, \pi^+)^{13}C$(ground state) can be reproduced by adjusting the cut-off mass Λ. We have checked whether the situation is similar in the reaction leading to the low-lying excited state of ^{13}C. Figs.17 and 18 show the calculated cross section for $^{12}C(p, \pi^+)^{13}C$ (3.09MeV;1/2$^+$) and $^{12}C(p, \pi^+)^{13}C$(6.86MeV;5/2$^+$) under different assumptions. (The transition leading to the 3.68MeV and 3.85MeV states are not separately observed.) As is seen in Figs.9, 16, 17 and 18, an overall agreement with the experimental data on (p, π^+) reactions is obtained by choosing the cut-off mass, $\Lambda \approx 700$–1000 MeV. Strictly speaking, the calculated cross section must be multiplied by the spectroscopic factor, which is slightly less than unity for the ground and the first excited state of ^{13}C. This does not, however, change the present discussions.

In the reaction $^{12}C(p, \pi^+)^{13}C$(6.86MeV;5/2$^+$) ,however, the theoretical values are about 10 times larger than the experimental data, when the cut-off mass Λ = 1GeV is adopted (Fig.18). Because the 6.86MeV level has the dominant configuration of $1d_{5/2}$ or $2s_{1/2}$ particle coupled to the collective 2^+(4.43MeV) state of ^{12}C, the probability of the $1d_{5/2}$ particle coupled to the ^{12}C ground state is small and is estimated to be about 0.2 by Miller[13]. If we include this factor, the absolute values of the calculated cross section agree with those of experiment. Very recently, however, the theoretical investigation of ^{13}C by Meder and Purcell[38] show that the configurations of the $2s_{1/2}$ and $1d_{5/2}$ particles coupled to the 2^+ state of ^{12}C are dominant, while the probability of the $1d_{5/2}$ particle coupled to the ground state of ^{12}C is very small

(i.e. about 10^{-3}). If we admit their predictions, we encounter

large discrepancies between the theory and experiment. Here we must

notice that, in this case, it will not be allowed to calculate the pion

production by keeping only a very small matrix element of the neutron

transfer to $1d_{5/2}$ orbit. The neutron transfer to the $2s_{1/2}$ and $1d_{5/2}$

orbits coupled to the 2^+ state of ^{12}C,

$$p + {}^{12}C \begin{array}{c} \nearrow p + {}^{12}C(2^+) \searrow \\ \searrow \pi + {}^{13}C(d_{5/2} \otimes gr.) \nearrow \end{array} \pi + {}^{13}C(d_{5/2}, 2s_{1/2} \otimes 2^+), \qquad (6.4)$$
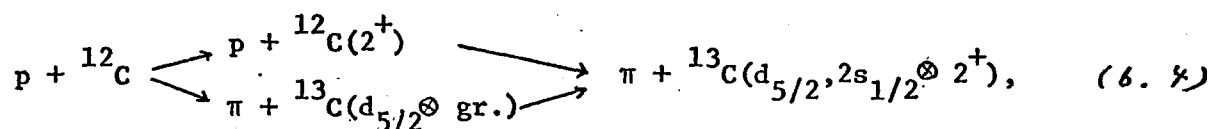
will dominate the exitation of $5/2^+$ level of ^{13}C. At present, it is

hard to draw a definite conclusion about the exitation of $5/2^+$ due to

the lack of reliable data on the spectroscopic factor of this level.

The effects of the two-step processes to the ground and the first excited

state of ^{13}C, are examined by Miller[13]. He showed that these are

minor corrections to the cross section, although they are not negligibly

small.

There is another approach to the (p, π^+) reaction without employing

the distorted waves. Dillig et al.[39] have studied the effects of

two-nucleon correlation in the framework of the Jastrow model. Grossman

et al.[40] have calculated the (p, π^+) reaction cross section by explicitly

including the pion production by two nucleons. There approaches are related

to ours through the effects of distorted wave, but the detailed

correspondences are not clear. We shall not discuss them further.

Finally we shall shortly discuss about the first-order Kisslinger-

potential. As was discussed in sections 5 and 6, the first-order

Kisslinger-potential fails to explain both the elastic and the (p, π^+)

reaction cross section. This is because the s-wave term is too small

and then the potential is strongly p-wave nature. The reason of this is

that the pion-nucleon s-wave scattering in the low energy is dominated

by the isovector type, while only the isoscalar part contributes to the

first-order optical potential for isospin-zero nucleus. On the other

hand, the best-fit potential to the elastic scattering has the strongly

repulsive s-wave term and is more close to the local potential. The

similar situation is also seen in the pion-nucleus scattering length

a^N in the isospin-zero nucleus.   Under the impulse approximation,

the pion-nucleus scattering length for isospin-zero nucleus is calculated

from the pion-nucleon scattering lengths a_1 and a_3 (a_{2T}) as,

$$a^N(impulse) = A \frac{a_1 + 2a_3}{3} \qquad (6.5)$$

Using the experimental values of a_1 and a_3 by Bugg et al.[41]),

$$a_1 = 0.170 \pm 0.004 \quad \mu^{-1}$$

$$a_3 = -0.092 \pm 0.002 \quad \mu^{-1} \qquad (6.6)$$

we calculate the pion-^{12}C scattering length as

$$a^N(impulse) = -0.056 \quad \mu^{-1} \qquad (6.7)$$

while the experimental value[42]) is

$$a^N(exp.) = -0.33 \pm 0.028 \quad \mu^{-1} \qquad (6.8)$$

Here, the theoretical value is too small to explain the experimental

data.

Previously Moyer and Koltun[43]) have calculated the multiple

scattering corrections (incoherent scattering and nucleon binding

corrections) to the pion-nucleus scattering length, which can account

for the major portion of the above disagreement. Firstly, we show the

importance of the nucleon-binding effects in a simple model-calculations,

according to the discussion by Hüfner [6]). The nucleon-binding correction

$\delta t = \tau - t$ is calculated by

$$\delta t = \tau - t = t(G - G_0)\tau \cong t(G - G_0)t, \qquad (6.9)$$

where G and G_0 are the many body and the two body Green functions

given in section 4. Adopting the Fermi-gas model, we incorporate the

Pauli-effects by

$$\langle p\mathbb{k} \mid G_p(E) \mid p\mathbb{k} \rangle = \frac{\theta(p - p_F)}{E - T_\pi - \frac{p^2}{2m_p} + i\mathcal{E}} \qquad (6.10)$$

where p and $\mathbb{k}$ are the momenta of the nucleon and the pion, respectively.

The nuclear Fermi momentum is denoted as p_F and the theta function

ensures that the excited nucleon is above the Fermi-surface. Further

the binding-energy correction of the nucleon is expressed as

$$\langle p\mathbb{k} \mid G_B(E) \mid p\mathbb{k} \rangle = \frac{1}{E + U_N(0) - T_\pi - (\frac{p^2}{2m_p} + U_N(p))} \qquad (6.11)$$

where $U_N(p)$ is the momentum-dependent nucleon potential and $U_N(0)$ is

the potential for the nucleon in the Fermi sea. We assume $U_N(p) \approx 0$.

In the low-energy limit $E = 0$ we can easily calculate the nucleon-

binding corrections in eq. (6.9). Noting that in the low-energy limit

$\langle \mathbb{k} p \mid t_{\pi N} \mid \mathbb{k}' p' \rangle = -\frac{1}{4\pi^2\mu}a$ in each eigenchannel, the nucleon-binding

correction δa^N in the pion-nucleus scattering length is given by

$$\delta a^N = -\frac{2}{\pi} a^2 p_F \qquad (Pauli\ correction\ ) \qquad (6.12)$$

and

$$\delta a^N = -a^2 \sqrt{2\mu \mid U_N(0) \mid} \ . \qquad (Binding\ energy\ correction) \qquad (6.13)$$

Then the correction to the impulse approximation is written as

$$a^N = a^N(impulse) - A \frac{a_1^2 + 2a_3^2}{3} [\frac{2}{\pi} p_F + \sqrt{2\mu \mid U_N(0) \mid}] \ . \qquad (6.14)$$

Assuming p_F = 250MeV and $U_N(0)$ = -50MeV, we get for ^{12}C

$$a^N = -0.42 \ \mu^{-1} \qquad (6.15)$$

The results seem to overestimate the nucleon-binding effects in such

a oversimplified model. By adding both of the above effects, some

double-counting arises. It is, however, important to recognize that

the second-order corrections in eqs. (6.12) and (6.13) are always negative.

The nucleon binding effects, therefore, are expected to enhance the

repulsive character of the s-wave term in the Kisslinger-potential.

Because we are concerned with the pion optical potential for kinetic energy about 30MeV, the incoherent scatterin corrections, namely the virtual excitation of the nucleus, are expected to be large. Especially, the excitation of the isospin T = 1 excited state, like giant dipole resonance, by the pion-nucleon isovector interaction will be important. Thus the strong repulsive force in the s-wave part of the Kisslinger potential, required to fit to the elastic scattering, can be understood qualitatively as the multiple scattering effects. As was shown in Figs.3 and 4, the first-order potential becomes to be close to the best-fit potential for the elastic scattering, with the increase of the pion energy. The s-wave part of the Kisslinger-potential, the strong repulsive nature and its energy dependence, is quite an interesting problem. The quantitative understanding of them is still an open problem.

7. Summary and conclusions

In the present thesis, we have performed a phenomenological analysis of the (p, π^+) reaction cross section on ^{12}C in the distorted wave approximation. In the previous analyses of the (p,π^+) reaction with the original Kisslinger-type pion optical potential, the calculated cross sections were one or two order of magnitudes too large compared with the experimental data. The local potentials also failed to explain the (p, π^+) reaction and the pion elastic scattering cross section consistently. The original Kisslinger-potential, however, has been succeeded to explain the pion elastic scattering in various nuclei, and has been widely applied to the analysis of the elastic or the inelasric scattering of the pion. Therefore it is substantially important to investigate the reason why the Kisslinger-potential fails in the (p, π^+) reaction. We have shown that the difficulty comes from the wrong off-shell behavior of the p-wave part of the Kisslinger-potential, which strongly enhances the high momentum component of the pion wave function. This is the reason why the calculated cross section of (p, π^+) reaction was too large in the previous analysis. In order to improve these points, we have adopted the Gaussian-type cut-off function to reduce the off-shell contribution of the p-wave pion-nucleon interaction in the original Kisslinger-model. As a result, a satisfactory agreement with the experimental data on both of the elastic scattering and the (p, π^+) reaction cross section is obtained by choosing the cut-off mass $\Lambda \approx 700$-1000 MeV. Thus, the (p, π^+) reaction offers us the

invaluable informations about the pion-nucleus interaction through the final state interactions. A systematic analysis of the (p, π^+) reaction on different nuclei is desirable, but the experimental data of elastic scattering in low energy are not so rich except for ^{12}C, and the determination of the phenomenological pion optical potential is difficult.

Apart from the (p, π^+) reaction, the problem of the pion optical potential at the low energy (pion kinetic energy $T_\pi \lesssim 70$ MeV) is not understood quantitatively, as yet. The failure of the first-order optical potential suggests the importance of the s-wave rescattering effects in the nucleus, but the theoretical understanding of them is insufficient. At present, the major interests about the pion-nucleus interaction are concentrated on the (3,3) resonance region. However, the much more efforts to study the low energy pion-nucleus optical potential are necessary for the thorough understanding of the pion-nucleus interaction. It is, therefore, highly desirable to perform the experiments of the low-energy pion-nucleus elastic scattering in various nuclei.

Acknowledgements

References

1. D. S. Koltun, "The interaction of pion with nuclei",
    Adv. Nucl. Phys., 1969 vol. 3 p.71

2. G. Backenstoss, Ann. Rev. Nucl. Sci. 20 (1970) 467

3. Proceedings of the international seminar on pion-nucleus
    interaction, Strassbourg, France Sept. 1971, Univ. of
    Strassbourg.

4. L. S. Kisslinger, "Meson-nucleus physics" Lecture note
    at Orsay, 1973-1974

5. M. M. Sternheim and R. Silber, "Meson-nucleus scattering at
    medium energies", Ann. Rev. Nucl. Sci. 24 (1974)

6. J. Hüfner, Phys. Rep. 21C (1975) 1

7. L. S. Kisslinger, Phys. Rev. 98 (1955) 761

8. E. Rost and P. D. Kunz, Phys. Lett. 43B (1973) 17

9. M. P. Keating and J. G. Wills, Phys. Rev. C7 (1973) 1336

10. S. Dahlgren, P. Grafström, B. Höistad and A. Åsberg,
    Nucl. Phys. A211 (1973) 243

11. S. Dahlgren, B. Höistad and P. Grafström, Phys. Lett. 35B (1971) 219

12. S. Dahlgren, P. Grafström, B. Höistad and A. Åsberg, Phys. Lett.
    47B (1973) 439 ; Nucl. phys. A204 (1973) 219 ; Nucl. Phys. A211
    (1973) 243 ; Nucl. Phys. A227 (1974) 245

13. G. A. Miller, Nucl. Phys. A224 (1974) 269

14. G. A. Miller and S. C. Phatak, Phys. Lett. 51B (1974) 129

15. R. H. Landau, S. C. Phatak and F. Tabakin, Ann. Phys. (N.Y.) 78
    (1973) 299

16. R. H. Landau and F. Tabakin, Phys. Rev. D5 (1972) 2746

17. G. F. Chew and F. E. Low, Phys. Rev. 101 (1956) 1570

18. A. Johansson, U. Svanberg and P. E. Hodgson, Ark. Fys. 19 (1961) 541

19. A. Johansson, U. Svanberg and O. Sundberg, Ark. Fys. 19 (1961) 527

20. R. Alphonce, A. Johansson and G. Tibell, Nucl. Phys. 4 (1957) 672

21. P. Hillman, A. Johansson and H. Tyrén, Nucl. Phys. 4 (1957) 648

22. M. L. Goldberger and K. M. Watson, Collision Theory (John Wiley and Sons Inc., New York 1964)

23. K. M. Watson, Phys.Rev. 89 (1953) 575

24. N. C. Francis and K. M. Watson, Phys. Rev. 92 (1953) 291

25. K. M. Watson, Rev. Mod. Phys. 30 (1958) 565

26. A. K. Kerman, H. McManus and R. M. Thaler, Ann. Phys. (N.Y.) 8 (1959) 551

27. M. Ericson and T. E. O. Ericson, Ann. Phys. (N.Y.) 36 (1966) 323

28. E. H. Auerbach, D. M. Fleming and M. M. Sternheim, Phys. Rev. 162 (1967) 1683

29. L. S. Kisslinger and F. Tabakin, Phys. Rev. C9 (1974) 188

30. J. F. Marshall and M. E. Nordberg,Jr., Phys. Rev. C1 (1970) 1685

31. J. F. Amann, P. D. Barnes, M. Doss, S. A. Dytman, R. A. Eisenstein and A. C. Tompson, Phys. Rev. Lett. 35 (1975) 426

32. L. D. Roper, R. M. Wright and B. T. Feld, Phys. Rev. 138 (1965) B190

33. T. Nishiyama and H. Ohtsubo, Prog. Theor. Phys. 52 (1974) 952

34. H. Crannel, Phys. Rev. 148 (1966) 1107

35. I. Sick and J. S. McCarthy, Nucl. Phys. A150 (1970) 631

36. P. P. Kane, Phys. Rev. 112 (1958) 1337

37. J. Raynal, M. A. Melkanoff and T. Sawada, Nucl. Phys. A101 (1967) 369

38. M. R. Meder and J. E. Purcell, Phys. Rev. C12 (1975) 2056

39. M. Dillig, H. M. Hofman and M. G. Huber, Phys. Lett. (1973) 484

40. Z. Grossman, F. Lenz and M. P. Locher, Ann. Phys. 84 1974) 348

41. D. V. Bugg, A. A. Carter and J. R. Carter, Phys. Lett. 44B (1973) 278

42. R. Seki and A. H. Cromer, Phys. Rev. 156 (1967) 93

43. L. Moyer and D. S. Koltun, Phys. Rev. 182 (1969) 999

Table Captions

Table I. The best-fit parameters to the 185 MeV proton-^{12}C elastic scattering cross section by Johansson et al.[18].

Table II. The parameters for the 30.2 MeV pion-^{12}C Kisslinger-potential. Set I is the best-fit value to the elastic scattering cross section by Marshall et al.[30]. Set II is the theoretical value given by the pion-nucleon phase shifts which are taken from the work by Roper et al.[32].

Figure Captions

Fig. 1. $^{12}C(p, \pi^+)^{13}C$ reaction cross section. The solid line is the

calculated cross section in the plane wave approximation.

The experimental values are taken from Dahlgren et al.[10]).

Fig. 2.   Coordinates of the initial and the final systems in the

(p, π^+) reaction.

Fig. 3.   The parameter b_0 of the Kisslinger-potential for ^{12}C.

The solid line is the theoretical values calculated by the

pion-nucleon phase shifts by Roper et al.[32]). The dots are

the best fit parameters for the pion elastic scattering

on ^{12}C, and are taken from the works of Auerbach et al.[28]),

Marshall et al.[30]), and Amann et al.[31]).

Fig. 4.   The parameters b_1 of the Kisslinger-potential for ^{12}C.

The solid line is the theoretical value calculated by the

pion-nucleon phase shifts by Roper et al.[32]). The dots are

the best fit parameters for the pion elastic scattering

on ^{12}C and are taken from the works of Auerbach et al.[28]),

Marshall et al.[30]), and Amann et al.[31]).

Fig. 5.   The nuclear density for ^{12}C. The curve A is calculated

by the harmonic-oscillator model with b = 1.64, and curve B

by the parameters w = 1 and b = 1.72 in eq. (4.33).

Fig. 6.   34.3 MeV pion elastic scattering cross section on ^{12}C.

Curve a is calculated with the Coulomb interaction by the

best-fit pion potential to 30.2 MeV elastic scattering

data (Set I). Curves b and c (d and e) show the cut-off

mass Λ-dependences of the elastic scattering cross section

with nuclear-density parameters w = 4/3 and b = 1.64 (w = 1

and b = 1.72) in eq. (4.33). Here, the Coulomb interaction

is neglected. The curve f is calculated by using the first-

order optical potential (Set II). The experimental data

are taken from Marshall et al.[30]) for 30.2 MeV data and Kane

[36]) for 31.5 MeV data.

Fig. 7. $^{12}C(p, \pi^+)^{13}C$(ground state) reaction cross section. Curves

a and b are calculated with and without the Coulomb interaction.

Here, the harmonic-oscillator model for the neutron bound

state is used. The experimental values are taken from ref.[10]).

Fig. 8. $^{12}C(p, \pi^+)^{13}C$(3.09 MeV:$1/2^+$) reaction cross section. The

curves a and b are calculated with and without the effects

of distortion in the proton wave function. The harmonic-

oscillator model for the neutron bound state is used. The

experimental values are taken from ref.[10]).

Fig. 9. $^{12}C(p, \pi^+)^{13}C$(ground state) reaction cross section. Curves

a, b,and c are calculated with the pion potential Set I

with off-shell cut-off masses $\Lambda = \infty$, 1GeV and 700MeV, respectively

Curves d and e are the results with cut-off mass Λ = 700MeV

and also with the nuclear recoil and the nuclear recoil plus

pion-nucleon vertex corrections,respectively. The curve f is

for the pion potential Set II. Here the harmonic-oscillator

model to the neutron bound state is adopted. The experimental

values are taken from ref.[10]).

Fig.10. The absolute value of the real part of pion optical potential

$\left| R_e \langle k' | V^{\ell}(E_\pi(k_0)) | k \rangle \right|$ for angular momentum ℓ = 0 and $k_0 = k' =$

100MeV. The parameters Set I is employed. Curves a, b and c

are calculated with off-shell cut-off masses $\Lambda = \infty$, 1GeV and

700MeV, respectively.

Fig.11. The absolute value of the real part of pion optical potential

$\left| Re\langle k'| \ v^{\ell}(E_{\pi}(k_0)) \ | \ k \rangle \right|$ for angular momentum $\ell = 1$ and $k_0 = k' =$

100MeV. The others are the same as in Fig.10.

Fig.12. Radial wave function of the pion, in the momentum space with

angular momentum $\ell = 0$. Curves a and b are calculated by the

potential Set I with off-shell cut-off masses $\Lambda = \infty$ and 700MeV,

respectively. The curve c is the result by the first-order

pion optical potential.

Fig.13. Radial wave function of the pion, in the momentum space with

angular momentum $\ell = 1$. The others are the same as in Fig.12.

Fig.14. Radial wave function of the pion, in the coordinate space with

angular momentum $\ell = 0$. Curves A and B are calculated by the

potential Set I and Set II, respectively.

Fig.15. Radial wave function of the pion, in the coordinate space with

angular momentum $\ell = 1$. Curves A and B are calculated by the

potential Set I and Set II, respectively.

Fig.16. $^{12}C(p, \ \pi^+)^{13}C$(ground state) reaction cross section. Curves

a and b are calculated by the pion potential Set I with

off-shell cut-off masses $\Lambda = 1.5$GeV and 700MeV, respectively.

The parameters $w = 1$ and $b = 1.72$ for the nuclear density in

eq. (4.33) are used. The neutron bound state is taken to be

the Woods-Saxon type. Curve c is for the pion potential Set II.

The experimental values are taken from ref.[10].

Fig.17. $^{12}C(p, \ \pi^+)^{13}C(3.09MeV;1/2^+)$ reaction cross section. Curves

a and b are calculated by the pion potential Set I with

off-shell cut-off masses $\Lambda = \infty$ and 700MeV, respectively.

Curves c and d are for the potential Set I with cut-off mass $\Lambda = 700$MeV, and also with the nuclear recoil and nuclear recoil plus pion-nucleon vertex corrections, respectively. The curve f is for the potential Set II. In the above calculations, the harmonic-oscillator model for the neutron bound state is used. Curve e is the same as d but with nuclear-density parameters w = 1 and b = 1.72 in eq. (4.33), and the Woods-Saxon type for the neutron bound state. The experimental data are taken from ref.[10]).

Fig.18. $.^{12}C(p, \pi^+)^{13}C(6.86MeV;5/2^+)$ reaction cross section. Curves a, b and c are calculated by the pion potential Set I with off-shell cut-off masses $\Lambda = \infty$, 1GeV and 700MeV, respectively. Curve d is for the potential Set II. For the neutron bound-state wave function, the harmonic-oscillator model is used. The experimental data are taken from ref.[10]).

Table I

U	-16	MeV
W	-10	MeV
U_s	2.5	MeV
W_s	-1	MeV
a_i *)	0.5	fm
R_1	2.29	fm
R_2	3.07	fm
R_3	2.29	fm
R_4	3.07	fm

*) i = 1 - 4

Table II

	b_0 (fm^3)	b_1 (fm^3)
Set I	-4.41 + 0.14 i	5.26 + 0.18 i
Set II	-0.71 + 0.63 i	7.75 + 0.56 i

$\frac{d\sigma}{d\Omega}$ (nb/sr)

$^{12}C(P\,\pi^+)^{13}C$(ground state)

10^4

10^3

10^2

10

1

20   40   60   80   100   120   140
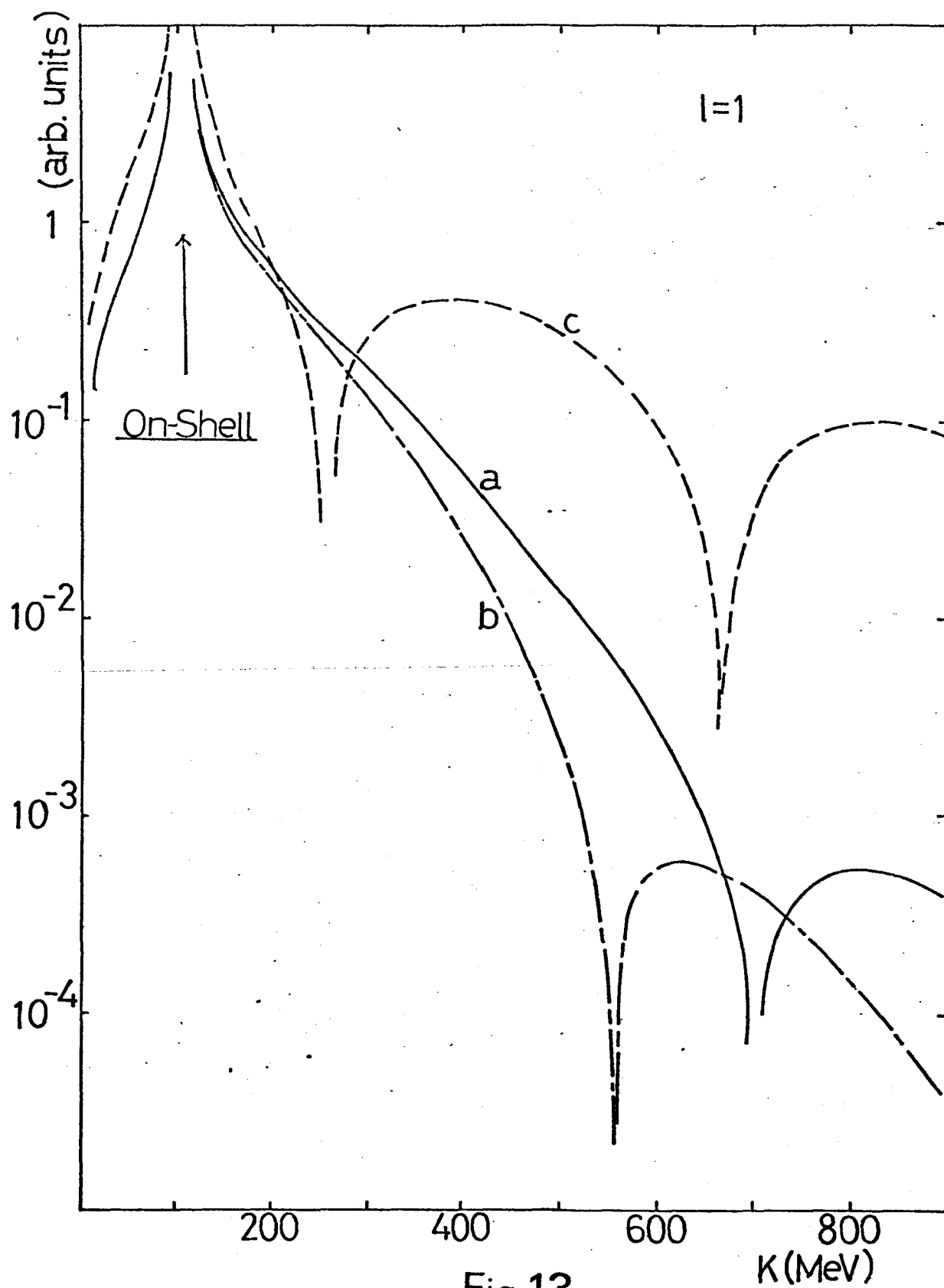
Fig.1

$\theta_{Lab.}$ (deg.)

Fig.2

Fig.3

Fig.4

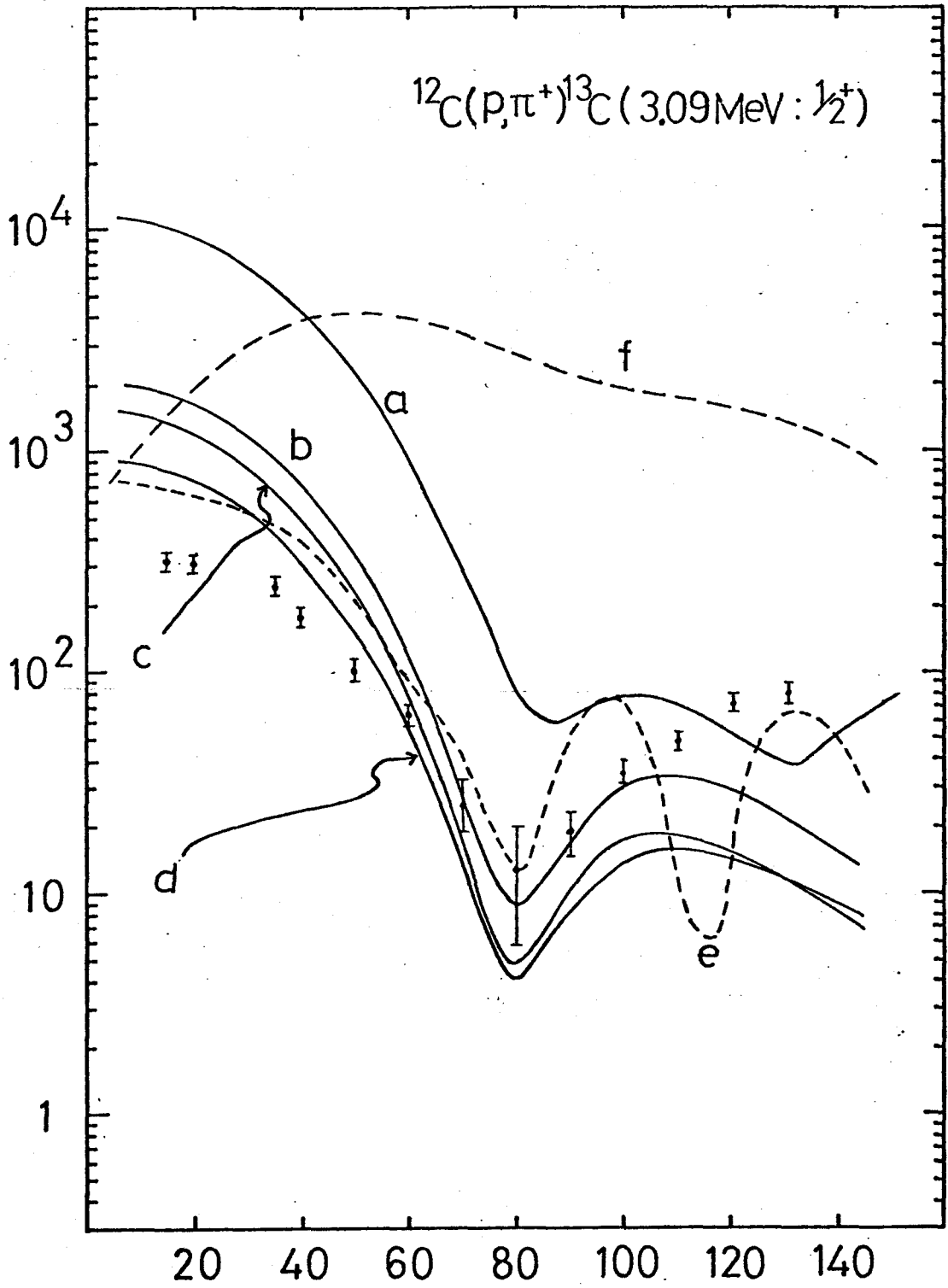Fig. 5

Fig.6

$\frac{d\sigma}{d\Omega}$ (nb/sr)

$^{12}C(p,\pi^+)^{13}C$ (Ground State)

b

a

Fig.7 $\theta_{Lab.}$ (deg.)

Fig.8

$\frac{d\sigma}{d\Omega}$ (nb/sr)

$^{12}C(p,\pi^+)^{13}C$ (Ground State)

10^4

f $X\frac{1}{10}$

10^3

$\Lambda=\infty$

a

10^2

b $\Lambda=1\,GeV$

c $\Lambda=700$

10

d   MeV

e

1

20   40   60   80   100   120   140

Fig.9 $\theta_{Lab.}$ (deg.)

$$|Re \langle K'|V^l(E_\pi(K))|K\rangle|$$
$$l=0 \qquad K=K'=100\,MeV$$

On-Shell

a

b

c

$\Lambda=\infty$

$\Lambda=1\,GeV$

$\Lambda=700\,MeV$

Fig.10

Fig.11

Fig.12

Fig.13

Fig. 14

Fig.15

Fig.16

Fig. 17

Fig.18